EFFECT OF HYDROSTATIC LOADING ON THE PORE STRUCTURE AND TRANSFER PROPERTIES OF A TIGHT GAS SANDSTONE

Yi WANG(1), Catherine DAVY(1), Franck AGOSTINI(1), Frédéric SKOCZYLAS(1), Laurent JEANNIN(2)
(1): LML UMR CNRS 8107/Ecole Centrale de Lille, CS20048,
59651 Villeneuve d'Ascq Cedex, France
(2): GDFSUEZ E&P International SA, 1 place Samuel de Champlain,
92930 Paris La Défense cedex - France

This paper was prepared for presentation at the International Symposium of the Society of Core Analysts held in St. John's, Newfoundland and Labrador, Canada, 16-21 August, 2015

ABSTRACT

Our study focuses on tight gas sandstones from a field located in North Africa and explored by GDFSUEZ E&P. This rock is characterized by its low porosity (below 10%) and its low absolute permeability (below 0.1mD i.e. $10^{-16}m^2$ under ambient conditions). A dedicated experimental setup has been designed to allow simultaneous measurements of gas permeability, connected porosity and poro-elastic properties, under given hydrostatic loading (up to 60 MPa). In the dry state, the decrease in accessible porosity is demonstrated experimentally: for one sample, accessible porosity is reduced by more than 10% (relative value) under 40 MPa hydrostatic loading. Simultaneously, gas permeability reduction is observed of a factor 8. In the partial water saturation state, the decrease in accessible porosity and effective gas permeability is enhanced. This shows an important stress sensitivity of the petrophysical properties of the sandstone: it is interpreted as pore entrapment under hydrostatic loading.

INTRODUCTION

Tight gas reservoirs are unconventional gas reservoirs constituted of low permeability sandstones, which are characterized by low connected porosity (lower than 10%), low absolute permeability (below 0.1mD i.e. $10^{-16}m^2$ under ambient conditions), and strong sensitivity to *in situ* stress as compared to conventional reservoirs [1-3]. Although these unfavorable properties make them more complicated to explore than conventional ones, tight reservoirs have a great potential in terms of gas production [4,5].

For their economical exploitation, characterization of the petrophysical properties of tight reservoirs is necessary. This paper presents the assessment of the effect of hydrostatic stress on the petrophysical properties of a particular sandstone, in both dry state and partially water-saturated state. We also relate the effect of hydrostatic stress to the changes in pore structure, by assessing the changes in connected pore volume.

Firstly, gas permeability and connected pore volume are investigated in the dry and in the partially water saturated state, under different confining pressures. Secondly, we compare variations in pore volume during loading and unloading to sample deformation, in order to confirm our interpretation of pore entrapment. Thirdly, we measure sandstone poro-elastic properties, in order to obtain a relationship between the externally applied stress and the drained bulk modulus K_b (or the solid matrix bulk modulus K_s). This allows getting further insight into the pore structure changes.

EXPERIMENTAL METHODS

Sample Preparation And Water Porosity Measurement

The samples of tight gas sandstone used in this study originate from a field located in North Africa [6], from depths between -2000 m and -2550 m. They are received by our laboratory as cylinders with a diameter of 37 mm, and a length cut to 60 mm.
Water porosity ϕ_w is defined as:

$$\phi_w = \left(m_{sat} - m_{dry}\right)/\left(\rho_w V_{sample}\right) \quad (1)$$

where m_{sat} and m_{dry} are respectively the water-saturated mass and the dry mass, ρ_w is water density and V_{sample} is the sample bulk volume. m_{dry} is obtained by oven-drying the sample at 105ºC, and regular weighing until the mass does not change by 0.01g for one whole week. Similarly, for m_{sat}, samples are water-saturated under vacuum until mass stabilization.

Partial Water Saturation State And Sample Conditioning

Partial water saturation S_w is defined as:

$$S_w = \left(m - m_{dry}\right)/\left(m_{sat} - m_{dry}\right) \quad (2)$$

In order to achieve a given S_w, a specific method is used, which corresponds to that recommended by RILEM [7], as follows. Firstly, sample water-saturated and dry masses are assessed; the dry sample is then water saturated until reaching the desired mass m. It is then sealed in three aluminium layers, and one layer of paraffin. Following this, it is kept in a climatic chamber at 40 ºC for at least 14 days, to allow water to have a homogeneous distribution in the sample.

Gas Permeability Measurement

Gas permeability of each sandstone sample is measured with the quasi-stationary fluid flow method [8,9]. The test is performed in a hydrostatic cell where the sample is sealed in a Viton Jacket (Figure 1). A buffer reservoir with a manometer is set up outside the hydrostatic cell between the source of gas and the sample. At first, when valve V_3 is closed and V_1, V_2 and V_4 are open, gas flows from the source of gas, *via* the buffer reservoir, until reaching a steady state. At steady state, the upstream side of the sample is

at pressure P_1, while the pressure on the downstream sample side P_0 is equal to the atmospheric pressure. Then, valve V_1 is closed at time $t = 0$, and we measure the time necessary for upstream gas pressure to decrease by ΔP_1 (ΔP_1 is less than one 1% of P_1). During Δt, gas is assumed to flow steadily at an average pressure $P_{mean} = P_1 - \Delta P_1 / 2$ on the upstream side, and the average volume flowrate is given by:

$$Q_{mean} = \frac{V_1 \Delta P_1}{P_{mean} \Delta t} \tag{3}$$

where V_1 is the buffer reservoir volume. Finally, gas permeability is given by simplified Darcy's law [10]:

$$K_x = \frac{\mu Q_{mean}}{A} \frac{2LP_{mean}}{\left(P_{mean}^2 - P_0^2\right)} \tag{4}$$

where L is sample length, A is its sectional area and μ is the dynamic viscosity of gas (here Argon is used with $\mu = 2.2 \cdot 10^{-5} Pa \cdot s$).

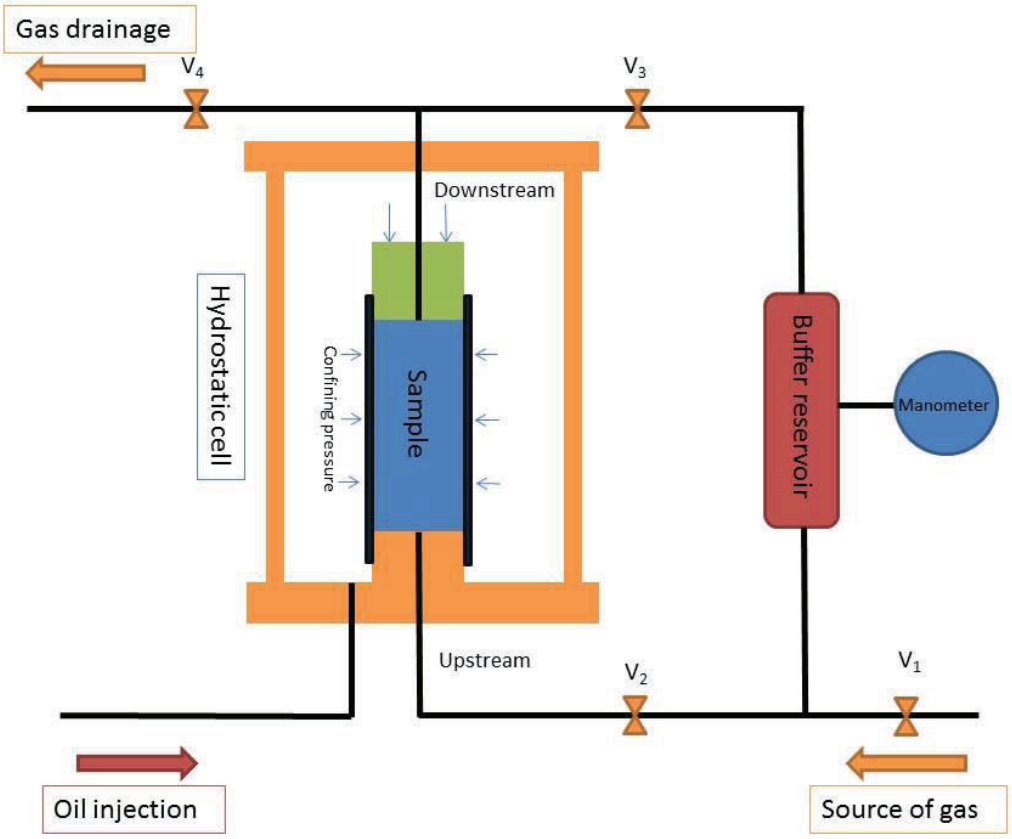

Figure 1 Principle for the quasi-stationary fluid flow method for gas permeability measurement

Measurement of Gas-accessible Pore Volume

This test quantifies the accessible pore volume under a given confining pressure [11,12]. The interpretation of this method is based on the ideal gas law:

$$PV = nRT \tag{5}$$

As shown in Figure 1, the sample is placed in the hydrostatic cell under given confining pressure. The buffer reservoir, of known volume Vr, is isolated from the rest of the circuit (by closing valves V_2 and V_3), and it is filled with gas at an initial pressure $P_{initial}$ (this is achieved by closing valve V_1 when reaching the desired pressure) while the sample is at atmospheric pressure. While valve V_4 is closed, the opening of valves V_2 and V_3 connects the buffer reservoir to the sample by both ends, while all other valves (V_1 and V_4) remain closed. From this moment, gas enters the sample connected pores and pressure P measured in the buffer reservoir decreases until reaching stabilization at a value P_{final}. Owing to the conservation of the gas mass initially located in the buffer reservoir, the relationship between $P_{initial}$ and P_{final} writes:

$$P_{initial}Vr = nRT = P_{final}\left(Vr + V_{pore}\right) \tag{6}$$

So that the accessible pore volume is determined by:

$$V_{pore} = \left(\frac{P_{initial}}{P_{final}} \quad 1\right)V_r \tag{7}$$

If the sample is in the dry state, the porosity accessible to gas is deduced as:

$$\phi_g = \frac{V_{pore}}{V_{sample}} \tag{8}$$

where V_{pore} is calculated by Equation (7) and sample volume V_{sample} is determined by hydrostatic weighing (using Archimedes' law): first, the dry sample is weighted, then it is submerged in water, and its weight under water (equal to its dry weight minus the weight of water occupying the volume of the sample) is measured. Sample volume is the difference between the two weights divided by the density of water.

Poro-Elastic Property Measurement

The measurement of poro-elastic properties is based on the theory of Biot [14]. The saturated porous material is considered as the superposition of two continua: the solid matrix and the fluid present in the pores. In the following, in a first approach, the porous medium (solid matrix+pores) is considered isotropic.

The drained bulk modulus K_b represents the deformability of the whole material i.e. of the so-called solid skeleton. The solid skeleton is constituted of connected and non-connected pores, and of the solid matrix [13]. K_b is measured under constant pore pressure (often equal to atmospheric pressure, as used here), by varying the hydrostatic stress by a small ΔP_c, so that K_b is given by:

$$K_b = \frac{\Delta P_c}{\Delta \varepsilon_{v1}} \tag{9}$$

where $\Delta \varepsilon_{v1}$ is the volumetric strain variation due to the variation in confining pressure ΔP_c.

The solid matrix bulk modulus K_s represents the rigidity of the solid matrix, which is composed of the solid and of the non-connected porosity alone [14]. In order to determine directly K_s, the variation in sample volumetric strain $_v$ is measured when the same variation in interstitial pore pressure p and in confining pressure $P_c = p$ is achieved:

$$K_s = \frac{p}{_v} \tag{10}$$

However, in order to avoid dealing with equal gas and confining oil pressures (which would mean extensive test leakage) , $\Delta p = \Delta P_c$ may be difficult to obtain. K_s is rather calculated from the measurement of modulus *H*, which is by varying pore pressure by an amount Δp when hydrostatic stress is kept constant [11-13], as:

$$H = \frac{\Delta p}{\Delta \varepsilon_{v2}} \tag{11}$$

where $\Delta \varepsilon_{v2}$ is the volumetric strain variation due to the variation in pore pressure Δp.
Finally K_s is given by [11-13]:

$$\frac{1}{K_s} = \frac{1}{K_b} - \frac{1}{H} \tag{12}$$

Generally, strain gauges are used to measure sample longitudinal and radial deformations. In this study, four LVDT sensors are used to measure longitudinal strains (Figure 2). As our sandstone samples are considered isotropic, the volumetric deformation ε_v is calculated by:

$$\varepsilon_v = \frac{3}{4}\left(\varepsilon_1 + \varepsilon_2 + \varepsilon_3 + \varepsilon_4\right) \tag{13}$$

When compared to strain gauges, using LVDT sensors has several advantages:

1) Sample length changes are measured directly without sample surface preparation and the assembly of the hydrostatic cell is simplified.
2) The problem of strain gauge bonding, especially on partially saturated samples is avoided.
3) The bonding of strain gauges and electric wire soldering can suffer from saturation/drying cycles, and from confining pressure changes.

4) By avoiding sample surface preparation and the use of glue, the measurement of sample mass variation before and after the experiment is more accurate.

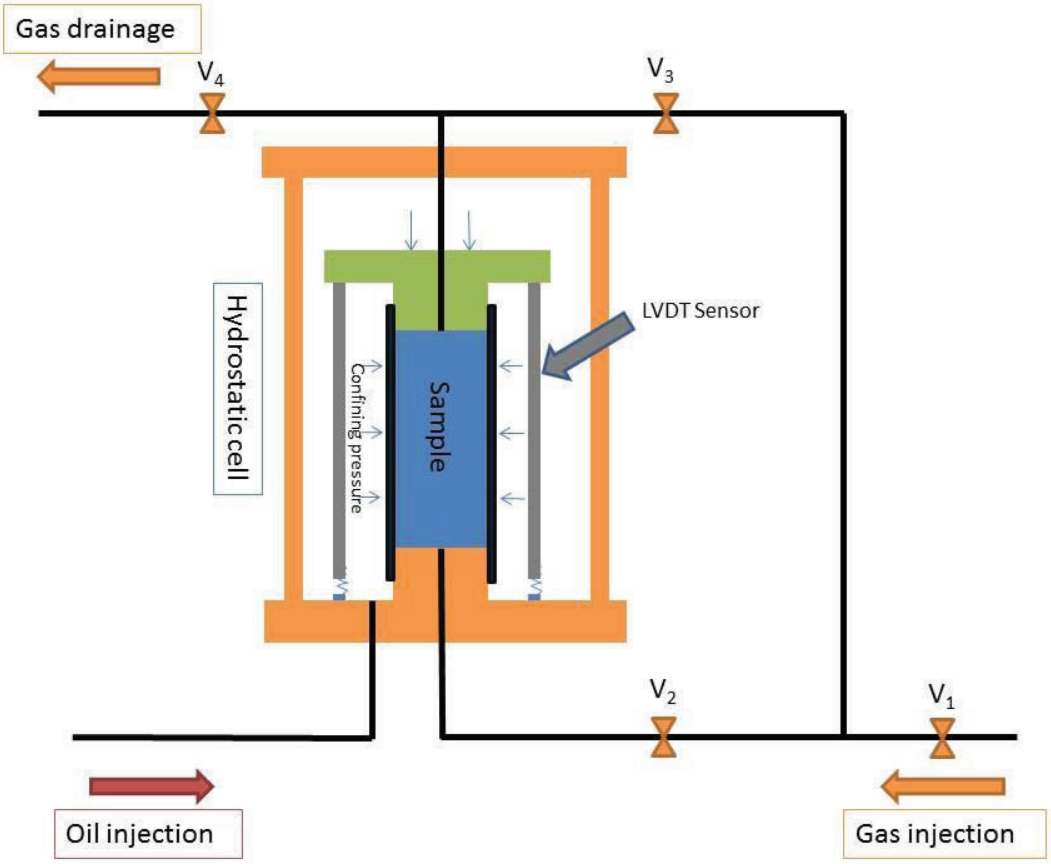

Figure 2: LVDT measurement system

RESULTS AND DISCUSSION

Water porosity

Water porosity results (Table 1) indicate that the tested samples have small water porosity values, with variations from 1.52% to 4.96%. No clear correlation is found between water porosity and drilling depth. This absence of correlation is expected [15, 17, 18]. Drilling depth has some influence on porosity, but it is not the determining factor: porosity also depends on diagenetic conditions (e.g. *in situ* chemical transformations of minerals) [6].

Table 1 Water porosity of tight sandstone samples

Number	2335	3248	3249	3250	3372	3375	3377	3379	4456	4458
Water porosity (%)	4.96	3.37	3.83	3.88	2.05	2.93	1.81	1.52	2.54	2.78
Depth (m)	2359	2181	2080	2197	2501	2496	2511	2516	2312	2311

Gas Permeability In The Dry State

Normalized dry gas permeability is defined as $K_{drynorm} = K(P_c)/K(P_c = 3MPa)$, where $K(P_c)$ is dry gas permeability under confining pressure P_c, $K(P_c = 3MPa)$ is that under confining pressure $P_c = 3MPa$. Figure 3 illustrates the evolution of normalized dry gas permeability over a range of confining pressures from 3 MPa to 40 MPa. A decrease in $K_{drynorm}$ by 90% is observed for the three samples presented in Figure 3, when hydrostatic stress reaches 40 MPa. This underlines the important stress sensitivity of the material. Samples 3249 and 3248 show almost the same type of $K_{drynorm}$ variation while 3379 seems to be more stress-sensitive. This is compared to the accessible porosity of those samples: samples 3249 and 3248 have comparable porosities (3.83% and 3.37% respectively), while sample 3379, which is more sensitive to P_c changes, has a lower porosity (of about 1.52%). This has already been observed in a previous study on tight Rotliegend sandstones from Germany [15].

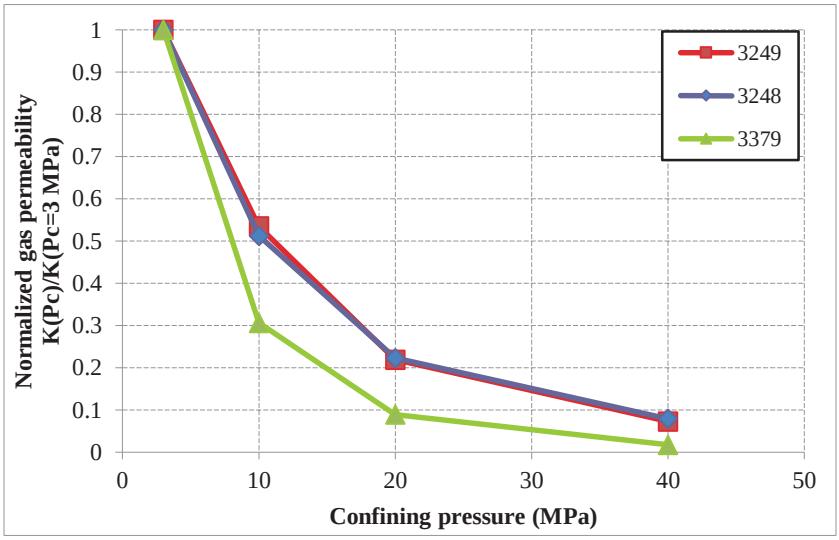

Figure 3: Normalized gas permeability for dry sandstone samples

Porosity And Pore Volume Variation In The Dry State

Similar stress-sensitivity is observed with normalized porosity, which is defined as $\phi_{norm} = \phi(P_c)/\phi(P_c = 3MPa)$ (Figure 4). Samples 3249 and 3248 lose nearly 10% of their porosity when confining pressure varies from 3 MPa to 40 MPa, while sample 3379 loses 25% of porosity. The loss of porosity is so large, that it is difficult to explain by the poro-elastic behaviour of the sandstone in terms of volume changes. It may well be indicative of the entrapment of pores in the solid skeleton.

To confirm this assumption, let us take sample 3248 as an example. The variation of pore volume as a function of sample volume variations (given by LVDT sensors) is shown in Figure 5. According to the poro-mechanics theory for isotropic media, a value of Biot coefficient equal to 1 implies that the variation in pore volume is identical to the variation

in sample volume: this is generally observed for granular media. For cohesive rocks such as tight sandstones, Biot's coefficient is smaller than 1, so that the variation in sample volume is greater than the variation in pore volume [14]. However, the reduction in pore volume is greater than the reduction in sample volume (Figure 5), even for moderate P_c (between 3 MPa and 10 MPa). This is explained by the closing of micro-cracks in the pore structure, which induces an occlusion of pores in the solid skeleton [12,15]. Above P_c = 10 MPa, accessible pore volume variation is parallel to the theoretical line corresponding to Biot's coefficient=1. Our interpretation is that micro-cracks are closed below P_c = 10 MPa: above this value, the material behavior is governed by its poro-elastic properties.

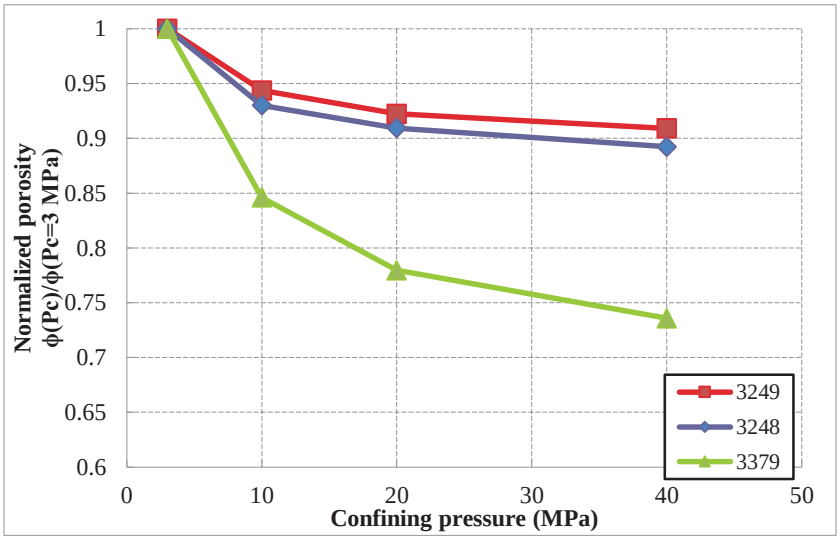

Figure 4 Normalized porosity for dry samples

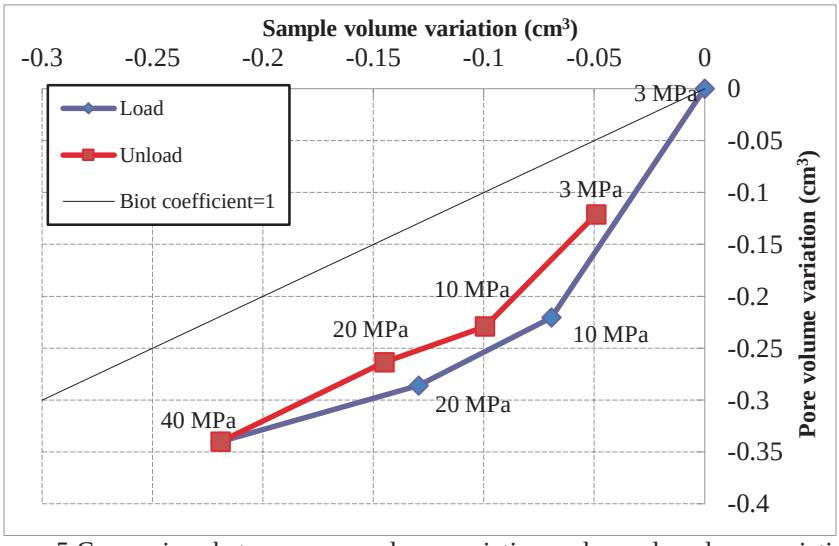

Figure 5 Comparison between pore volume variation and sample volume variation

Poro-elastic Properties In The Dry State

In order to confirm the changes in pore structure (entrapment under increasing P_c), poro-elastic properties K_b and K_s are assessed under different confining pressures. As shown in Figure 6, for the three samples, the effect of P_c is more important for low confinement. Between P_c = 3 and 10 MPa the increase in K_b reaches about 200%, and increases an additional 50% between P_c = 10 and 40 MPa. Finally at P_c = 40 MPa, K_b increases to about 20 GPa. Similar stiffness values are also observed for other such tight sandstones [14].

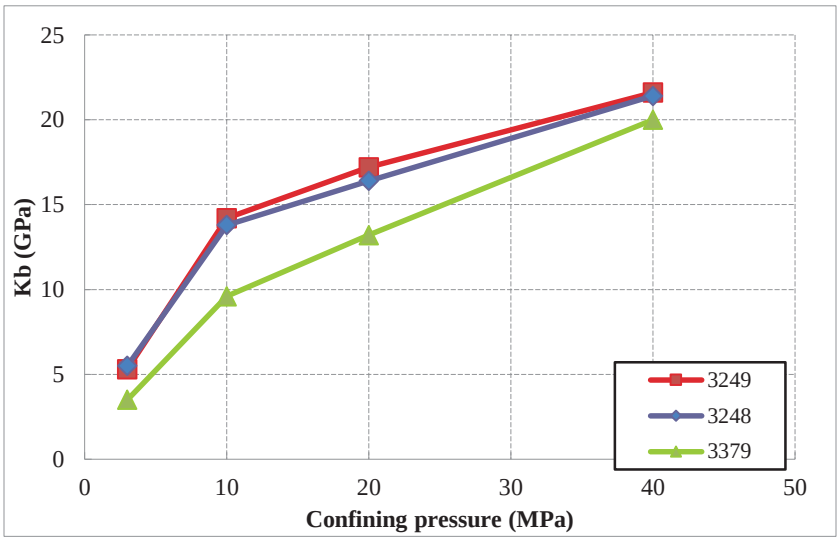

Figure 6 Drained bulk modulus K_b as a function of confining pressure

However, difficulties have been encountered when measuring the solid matrix bulk modulus K_s, which are quite high (above 20 GPa). When an interstitial pore pressure is applied, only small deformations of the solid matrix occur, which induces an important uncertainty to the measurement. Further effort shall be dedicated to accurately assess the value of K_s, as in [14].

Gas Permeability In A Partially Water Saturated State

In the partially water saturated state, normalized gas permeability is the ratio between gas permeability in the partially water saturated state at given P_c and gas permeability in the dry state at P_c =3MPa: $K_{norm} = K(P_c)/K(P_c = 3MPa)$. It is plotted under increasing confining pressure for sample 3249 in Figure 7. It is observed that K_{norm} is more stress-sensitive than in the dry state. For Sw = 25.6%, between P_c = 3 and 10MPa, normalized permeability has decreased significantly, by 70%. The sharp decrease continues until confining pressure reaches P_c = 20 MPa. Above this confining pressure value, normalized permeability shows little variation. This behavior is highly dependent on the structure of the pore network and on pore size distribution. The decrease in K_{norm} when P_c increases indicates that the pores, which have closed under increasing P_c, were significantly

participating in gas flow, so that they were not filled with water, although the material is in a partial water saturated state. Further interpretation will be conducted on this aspect with the help of Mercury Intrusion Porosimetry (MIP), Scanning Electron Microscopy (SEM) investigations and micro mechanical modelling [16].

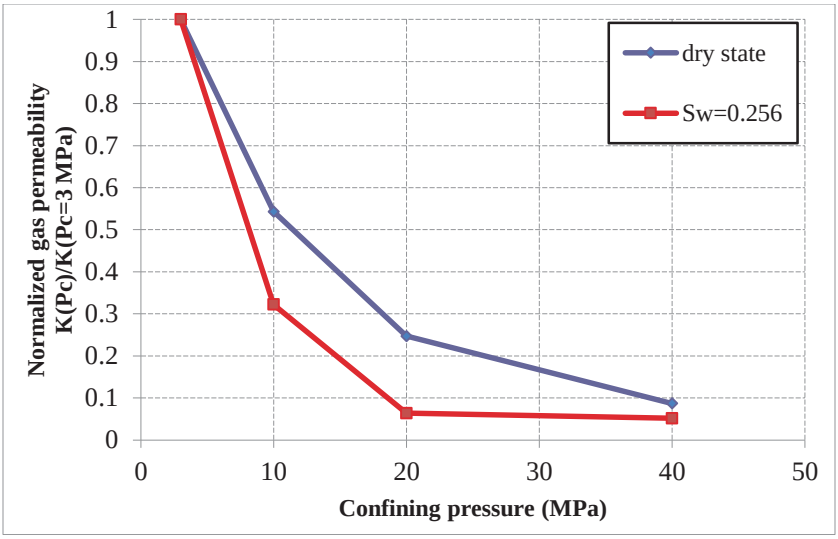

Figure 7 Normalized gas permeability of sample 3249 in the dry and partially water saturated states

Gas Accessible Pore Volume In A Partially Water Saturated State

The water saturation has a greater influence on gas-accessible pore volume, than on normalized permeability (
Figure 8). Large reductions are observed for Sw = 25.6%, especially when confining pressure P_c increases from 10 MPa to 20 MPa: a large portion of nearly 30% of the gas-accessible pore volume is lost.

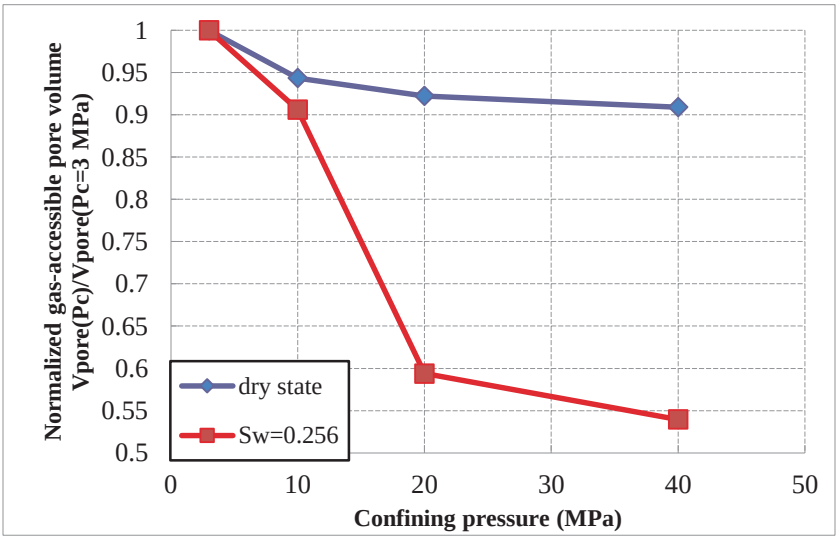

Figure 8 Normalized gas-accessible pore volume of sample 3249 in the dry and partially water saturated states

From Figure 7 and
Figure 8, we conclude that in the partially water saturated state, the evolution of permeability and gas-accessible pore volume do not evolve so smoothly as in the dry state: in the partially water saturated state, the major decrease in permeability occurs at the beginning of loading, while relative pore volume decreases mainly under intermediate confining pressures (10MPa to 20MPa). Further investigations and a dedicated micro-mechanical model are required for a proper interpretation.

CONCLUSION

This experimental study deals with samples from a tight gas reservoir. First, gas permeability is investigated under different confining pressures. For samples in the dry state, we show a great stress-sensitivity of normalized gas permeability. Additionally, sample 3379, with a smaller initial porosity, is more sensitive to external stress than the other two samples. The partial water saturation of the samples increases the sensitivity of permeability to changes in P_c. Secondly, gas accessible pore volume is measured under confining pressure. Large losses in pore volume are observed in dry state, which is attributed to pore entrapment, which occurs when micro-cracks close under increasing confining pressure. This phenomenon is more visible in a partially water saturated state. The variation in pore volume is compared with that of sample volume: under increasing P_c, a large loss of pore volume is observed, which is also an evidence of pore entrapment. Thirdly, poro-elastic experiments are conducted to provide further information on sample structure: it is observed that the drained bulk modulus K_b increases steadily under increasing P_c loading.

The interpretation of those tests requires further investigation. Rock micro-structure shall be assessed by Scanning Electron Microscopy (SEM) and Mercury Intrusion Porosimetry (MIP). The use of a micromechanical model will provide a prediction of petrophysical properties for the reservoir.

ACKNOWLEDGEMENTS

We gratefully acknowledge financial support by GDFSUEZ E&P International SA.

REFERENCES

1. Cluff, R. M., and A. P. Byrnes. "Relative Permeability In Tight Gas Sandstone Reservoirs-The ‘Permeability Jail’ Model." *SPWLA 51st Annual Logging Symposium*. Society of Petrophysicists and Well-Log Analysts, (2010).
2. Blasingame, T. A. "The characteristic flow behavior of low-permeability reservoir systems." *SPE Unconventional Reservoirs Conference. Keystone, Colorado, USA*. (2008).
3. Ward, J. S., and N. R. Morrow. "Capillary pressures and gas relative permeabilities of low-permeability sandstone." *SPE Formation Evaluation*, (1987) vol.2, no.03, 345-356.

4. Jiang, L. Z., J. Y. Gu, and B. C. Guo. "Characteristics and mechanism of low permeability clastic reservoir in Chinese petroliferous basin." *Acta Sedimentologica Sinica*, (2004) vol.22, no.1, 13-18.
5. Kang, Y. l., and P. Y. Luo. "Current status and prospect of key techniques for exploration and production of tight sandstone gas reservoirs in China." *Petroleum Exploration and Development*, (2007) vol.34, no.2, 239.
6. Tournier, F., et al. "Relationship between deep diagenetic quartz cementation and sedimentary facies in a Late Ordovician glacial environment (Sbaa Basin, Algeria)." *Journal of Sedimentary Research*, (2010) vol.80, no.12, 1068-1084.
7. Hilsdorf, H. K., and J. Kropp. "Permeability of Concrete as a criterion of its durability." *Report of RILEM Technical Committee TC*, (1992) vol.116.
8. Skoczylas, F., *Ecoulements et couplages fluide-squelette dans les milieux poreux: études expérimentales et numériques*., Dissertation, (1996).
9. Meziani, H., and F. Skoczylas, "An experimental study of the mechanical behaviour of a mortar and of its permeability under deviatoric loading." *Materials and structures*, (1999) vol.32, no.6, 403-409.
10. Davy, C. A., F. Skoczylas, P. Lebon, Th. Dubois, "Permeability of macro-cracked argillite under confinement: gas and water testing." *Physics and Chemistry of the Earth*, (2007) vol.32, no.8, 667-680.
11. Chen, X. T., *Effet du chauffage sur le comportement mécanique et poro-mécanique de matériaux cimentaires: propriétés hydrauliques et changements morphologiques*., PhD Dissertation, (2009).
12. Chen, X. T., G. Caratini, C. A. Davy, D. Troadec, F. Skoczylas, "Coupled transport and poro-mechanical properties of a heat-treated mortar under confinement." *Cement and Concrete Research*, (2013) vol.49, 10-20.
13. Coussy, O., *Poromechanics*. John Wiley & Sons, Chichester, (2004).
14. Duan, Z., C. A. Davy, F. Agostini, L. Jeannin, D. Troadec, F. Skoczylas "Gas recovery potential of sandstones from tight gas reservoirs." *International Journal of Rock Mechanics and Mining Sciences*, (2014) vol.65, 75-85.
15. Fu, X., *et al.* "Effect of mechanical loading and water saturation on the gas recovery of tight gas: experimental study." *2012 International Symposium of the society of Core Analysts*. Aberdeen, SCA, (2012), 27-30.
16. Dormieux, L., L. Jeannin, and N. Gland. "Homogenized models of stress-sensitive reservoir rocks." *International Journal of Engineering Science*, (2011) vol.49, no.5, 386-396.
17. Ramm, M., and K. Bjørlykke, 1994, Porosity/depth trends in reservoir sandstones: Assessing the quantitative effects of varying pore-pressure, temperature history and mineralogy, Norwegian shelf data: Clay Minerals, v. 29, p. 475 – 490.
18. Ehrenberg S. N., Nadeau P. H., Sandstone vs. carbonate petroleum reservoirs: A global perspective on porosity-depth and porosity-permeability relationships, AAPG Bulletin, v. 89, no. 4 (April 2005), pp. 435 – 445.